Research Article | Vol. 26, No. 17 | 20 Aug 2018 | OPTICS EXPRESS 21558
Optics EXPRESS

Dynamic-grating-assisted energy transfer between ultrashort laser pulses in lithium niobate

STEFAN NOLTE,[1] BJOERN BOURDON,[1] FELIX FREYTAG,[1] MIRCO IMLAU,[1,*] ALEXANDR SHUMELYUK,[2] AND SERGUEY ODOULOV[2]

[1]*Department of Physics, Osnabrueck University, Barbarastrasse 7, D-49076 Osnabrueck, Germany*
[2]*Institute of Physics, National Academy of Sciences, 03650 Kyiv, Ukraine*
[*]*mimlau@uni-osnabrueck.de*

Abstract: Energy redistribution between two subpicosecond laser pulses of 2.5 eV photon energy is observed and studied in congruent, nominally undoped $LiNbO_3$, aiming to reveal the underlying coupling mechanisms. The dependences of pulse amplification on intensity, frequency detuning and pulse duration point to two different contributions of coupling, both based on self-diffraction from a recorded dynamic grating. The first one is caused by a difference in pulse intensities (transient energy transfer) while the second one originates from a difference in pulse frequencies. The latter appears when chirped pulses are mutually delayed in time. A quite high coupling efficiency has been observed in a 280 µm thin crystal: one order of magnitude energy amplification of a weak pulse and nearly 10% net energy enhancement of one pulse for the case of equal input intensities.

1. Introduction

The intensity coupling of two light waves that propagate in a nonlinear medium (two-beam coupling) is one of the basic phenomena of dynamic holography [1]. This type of coupling has attracted the interest of researchers since the discovery in 1980's of unidirectional intensity transfer between two waves that are recording a shifted phase grating in a nonlinear optical crystal (see, e.g., [2, 3]). A new type of coherent light wave amplification became possible, various dynamic-grating-based coherent optical oscillators were designed and used as self-starting phase conjugate mirrors [4].

In the early stage of the dynamic holography, emphasis was put on the intensity coupling of continuous waves (cw), both in theory and in experiment. Quite quickly the developed approaches were extended for the description of the interaction of light pulses. The term "two-beam coupling" was still used to define the interaction of pulses (see, e.g., [5–7]), but it became often replaced by "pulse energy transfer" [8–12] or "energy exchange" [13]. The researchers dealing with pump-probe techniques were facing the problem of so called "coherent peaks" [14, 15], which is a consequence of pump and probe pulse coupling via a dynamic grating, too [16]. It should be mentioned that the fundamental phenomenon of gain in stimulated Rayleigh-wing scattering had been treated well before the appearance of femtosecond lasers [17–21], but never in terms of diffraction from a grating. A comprehensive analysis of pulse coupling is given in the review article [22] and textbooks [23, 24]. More than a hundred original publications that consider different aspects of grating-assisted interaction of pulses have been published.

The self-diffraction of the recording pulses themselves, or diffraction of an auxiliary probe pulse from the developing instantaneous or inertial grating, are still studied nowadays [25]. It has been used for the characterization of the pulses themselves [26, 27], plasma filament control in air [6] and nonlinear liquids [11], nonlinear spectroscopy of the materials themselves [7, 13], frequency conversion [28, 29], etc. The subpicosecond pulses even allowed, quite counter-intuitively, for grating recording with light being strongly nondegenerate in frequency [30]. Both, dynamic

#330440 https://doi.org/10.1364/OE.26.021558
Journal © 2018 Received 26 Apr 2018; revised 9 Jul 2018; accepted 9 Jul 2018; published 7 Aug 2018

Optics EXPRESS

and permanent gratings were recorded. The recording of static holograms with image bearing pulses proved to be possible with subpicosecond pulses of different color, with further image reconstruction by a cw laser beam [30].

Commonly, the description of grating-assisted pulse interaction is based on the solution of coupled wave equations for a spatial variation of slowly varying complex amplitudes (see, e.g., [2, 3, 22–24]). While these equations are nearly always the same, the material equations, which are necessary to calculate the temporal dynamics of interaction, depend on the particular nonlinear medium and the particular type of nonlinearity involved. The present work is an experimental study in which the measured dependences are compared with predictions of already existing theories that describe particular coupling processes. We conduct this study to estimate the strength of the coupling of subpicosecond pulses in $LiNbO_3$ and to reveal the types of underlying wave mixing process(es) that is (are) responsible for an energy redistribution between the interacting pulses. Lithium niobate was the first crystal in which a photorefractive nonlinearity and grating-assisted intensity redistribution of the recording waves have been discovered [4, 31]. Apart from the instantaneous high-frequency Kerr nonlinearity [32] and two-photon absorption (TPA) nonlinearity [33], several inertial nonlinear responses have been revealed, too. They include photoexcitation of free carriers [34, 35], and the formation of various kinds of polarons [36]. The identification of the physical process of nonlinearity that is responsible for the investigated pulse coupling will be, however, the topic of a separate study.

The structure of the present paper is as follows. After this *Introduction*, the section *Experimental technique* presents the description of chirped femtosecond laser pulses, the nonlinear optical crystal itself, and the experimental setup. The third section, the *Experimental results*, consists of four parts, devoted to particular sets of measurements. In subsection 3.1 a small signal amplification is studied, with a weak probe pulse which interacts with a stronger pump pulse, both pulses being perfectly matched in time. Subsection 3.2, on the opposite, focuses on the interaction of pulses of equal energies that become detuned in frequencies being temporally mismatched. In subsection 3.3 the effect of the pulse duration is analyzed for the interaction of identical pulses. Finally, in the last subsection 3.4, a possible influence of extended temporal spectra of ultrashort pulses on their energy coupling is analyzed. In the *Discussion* section it is shown that the major contribution to energy transfer between subpicosecond pulses in congruent, nominally undoped $LiNbO_3$ is due to two different coupling processes: (*i*) quasi steady-state coupling of waves of equal intensity with mutually shifted frequencies and (*ii*) transient, non-steady-state coupling of waves of different intensities but with identical spectra. The first process was already proven to be responsible for the interaction of frequency-chirped pulses in gases, plasma and liquids (see, e.g., [6, 7, 11, 13]). Our study shows that it results in a quite strong pulse interaction in a solid-state material as well. The second process has never been considered, to the best of our knowledge, for the interaction of short pulses in spite of the fact that it was revealed long ago for interactions in photorefractive crystals [37] and media with a thermal nonlinearity [38, 39].

2. Experimental technique

All experiments in this paper are performed with a classical interaction geometry of two-beam coupling of co-propagating light beams which is also standard for pump-probe techniques. Figure 1 shows schematically the experimental setup used for our studies. Two ultrashort light pulses with equal central wavelengths of $\lambda = 488\,\mathrm{nm}$ (or $\lambda = 590\,\mathrm{nm}$) impinge upon a $LiNbO_3$ sample with a full crossing angle in air of $2\theta < 5°$. A relatively small angle can be set by the use of a single focusing lens (L) for both pulses to ensure a good spatial overlap of the femtosecond pulses. An optical delay line (DL) is installed in one of the two beams to adjust a temporal mismatch Δt between both pulses of up to several picoseconds.

The main measured characteristic in this paper is the normalized transmission $T_i = W_i/W_i^0$ for each of the two interacting pulses (subscripts pu and pr for pump and probe pulses, respectively).

Optics EXPRESS

Here, W_i denotes the transmitted pulse energy of one pulse in presence of the other pulse, while W_i^0 is the energy of the unaffected transmitted pulse, with no other pulse in the sample. The transmission T_i is measured as a function of different experimental parameters: total intensity of the two pulses I, pulse intensity ratio $R = I_{pu}/I_{pr}$, temporal delay between the two pulses Δt, and FWHM pulse duration τ_c. These data make it possible to evaluate a weak-probe gain G_{wp} (when the probe pulse propagates in presence of a stronger pump pulse) and a strong-probe gain G_{sp} (in case of energy transfer between pulses with equal energies), as it is explained in the next sections. The energies of the incident and transmitted pulses are measured with a laser power meter (*Coherent LabMax*) as well as biased silicon detectors (*Thorlabs DET10A*).

The y-cut sample of congruent, nominally undoped lithium niobate with plane parallel input/output faces has a thickness of $d \approx 280\,\mu m$. At the particular wavelength of $\lambda = 488\,nm$ the pronounced two-photon absorption and small polaron absorption have been reported [36,40]; the coefficients of two-photon absorption, $\beta_{TPA} \simeq 5.6\,mm/GW$, and optical Kerr effect, $n_2 \simeq 5 \cdot 10^{-20}\,m^2/W$, are known from z-scan experiments [40].

The femtosecond pulses are generated by a mode-locked Ti:Sapphire laser (*Coherent, Libra*) that feeds two independently tunable Optical Parametric Amplifiers (OPA, *Coherent, OPerA-Solo*) [29, 30]. Pulses with central wavelengths of $\lambda = 488\,nm$ and spectral bandwidths of $\Delta\lambda = 4.7\,nm$ from only one OPA are used for frequency non-degenerated experiments, unless otherwise stated. The central wavelength and spectral bandwidth of the interacting pulses are monitored with a fiber spectrometer (*Ocean Optics, USB4000*).

To evaluate the peak intensity $I_{pu,pr}$ of a pulse with an energy W, its spatial and temporal profiles need to be known. Measurements of the transverse intensity distribution at the sample input face revealed a Gaussian-like shape of both beams with nearly identical radii of $r \approx 55\,\mu m$ at the e^{-2} level of the peak intensity. The durations τ_c of the incident pulses are estimated with a commercial autocorrelator (*APE, pulseCheck PD15*) assuming a Gaussian temporal intensity profile with peak value:

$$I = \sqrt{\frac{16\ln(2)}{\pi^3}}\frac{W}{r^2\tau_c}\,. \tag{1}$$

The pulse energies W (and therefore the peak intensities I) of the two pulses were controlled by using variable neutral density filters (VFs) so that different ratios $R = I_{pu}/I_{pr}$ could be adjusted. The pulse duration could be changed within a range of $\tau_c = (80 - 830)\,fs$ using a pulse

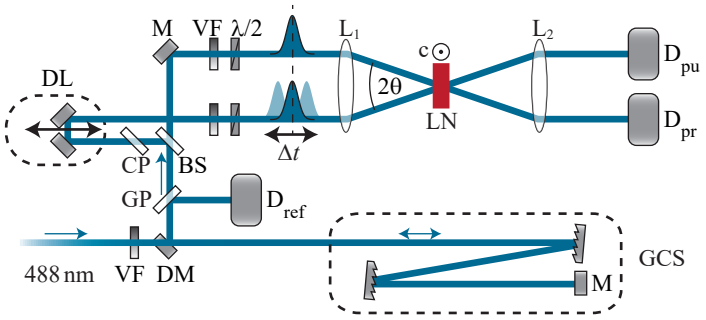

Fig. 1. Schematic of the experimental setup: variable neutral density filter (VF), double grating compressor/stretcher (GCS), glass plate (GP), 50/50 beamsplitter (BS), compensator plate (CP), optical delay line (DL), mirror (M), D-shaped mirror (DM), $\lambda/2$-waveplate, lenses $f = 500\,mm$ ($L_{1,2}$), full crossing angle in air 2θ, lithium niobate sample (LN) with the polar **c**-axis normal to the plane of drawing, and silicon detectors (D_{ref}, D_{pu} and D_{pr}).

Optics EXPRESS

compressor/stretcher (GCS). A folded double-grating setup allows for introducing a negative pulse chirp in our experiment. Otherwise, a double prism setup could be used to impose a positive pulse chirp, profiting from the material dispersion (N-SF11 glass, for example).

The spectral bandwidth $\Delta\omega = 3.7 \cdot 10^{13}$ rad/s of the Gaussian shaped pulses defines the theoretically smallest, Fourier-transform-limited pulse duration of $\tau_0 = 75$ fs. For deliberately stretched pulses the frequency chirp coefficient $\dot{\omega}$ depends on the pulse duration τ_c (cf. [41]):

$$\dot{\omega} = (\Delta\omega/\tau_c)\sqrt{1-(\tau_0/\tau_c)^2}. \tag{2}$$

The total peak intensity $I = I_{pu} + I_{pr}$ never exceeded 640 GW/cm^2 to avoid laser-induced damage of the sample. The kHz repetition rate of the pulse train was reduced by an optical chopper to 12.5 Hz. All coupling processes under investigation emerge in a single pulse shot and no cumulative effects have been observed for repetitive-rate operation. This enabled us to average data of 200 consecutive pulses to reduce the impact of pulse-to-pulse fluctuations and to improve accuracy.

Both interacting pulses enter the sample in a plane perpendicular to the axis of spontaneous polarization $\mathbf{c}$. The light polarization could be adjusted to each beam independently by two $\lambda/2$ phase retarders, with care taken to avoid possible changes in the temporal delay Δt between the pulses. Usually, the polarization unit vectors are set parallel to the polar axis, $\mathbf{e}_1 \parallel \mathbf{e}_2 \parallel \mathbf{c}$, unless stated otherwise. This particular configuration excludes a possible contribution to pulse coupling from the space charge field grating because the relevant Pockels tensor components of $LiNbO_3$ are vanishing (see, e.g., [42]).

3. Experimental results

3.1. Coupling of pulses with different energies

We start from the description of experiments with pulses of significantly different energies that allow to characterize a weak-probe gain G_{wp}. Figure 2 gives a typical example of the probe pulse transmission in presence of a pump pulse with the same polarization $T_\parallel$ as a function of the temporal delay Δt between both pulses (black data points). The pulse duration of each pulse $\tau_c \approx 80$ fs is close to the Fourier limit τ_0. The transmission $T_\parallel(\Delta t)$ features a considerable increase in the vicinity of $\Delta t = 0$ with a maximum value of $T \approx 2.3$. An asymmetry of the signal

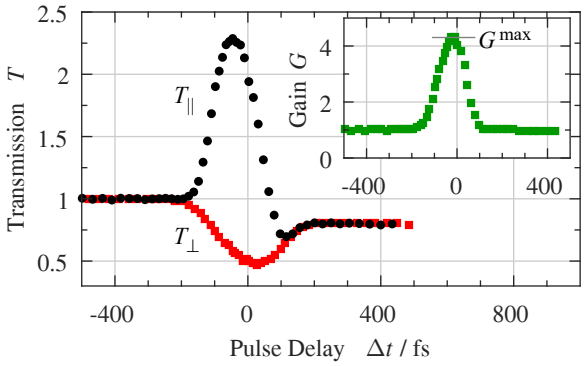

Fig. 2. Pulse delay dependence of the normalized probe pulse transmission with parallel ($T_\parallel$, black dots) and orthogonal polarization ($T_\perp$, red squares). The inset shows the gain G (green squares) evaluated from Eq. (3). The total peak intensity of the two pulses is $I \approx 635$ GW/cm^2 with a peak intensity ratio of $R \approx 100$, pulses duration of $\tau_c = (80 \pm 5)$ fs and beam radii of $r = (55 \pm 5)$ µm.

Optics EXPRESS

$T_{\parallel}(\Delta t)$ is obvious, with the transmission saturated at $T_{\parallel}^{\mathrm{sat}} \approx 0.8$ for large positive Δt. This value of $T_{\parallel}^{\mathrm{sat}}$ below unity can be attributed to the light-induced absorption caused by optically generated small, strong-coupling polarons [33, 36].

It is noteworthy that the appearance of additional oblique beams behind the sample has been detected within the Δt interval where probe amplification occurs ($T \geq 1$) . Their angular position suggests that these are higher orders of diffraction from a grating recorded with the two incident pulses. The largest overall energy of these higher diffraction orders could approach 10% of the total transmitted energy.

The transmission of the probe pulse changes dramatically if the polarization of the pump pulse is turned to 90°, as depicted by the red data points. Here, the transmission $T_{\perp}$ shows a dip in the vicinity of $\Delta t = 0$ that can be attributed to the effect of two-photon absorption [33]. In agreement with this assumption, we found that the temporal width of this dip depends on the duration τ_c of the incident pulses, while possible broadening of the dip caused by the group velocity mismatch can be neglected for the used thin birefringent crystal. The saturation is again reached at $T_{\perp}^{\mathrm{sat}} \approx 0.8$.

From the comparison of both curves in Fig. 2 one can deduce that in presence of the pump pulse with the same polarization the probe pulse experiences simultaneously attenuation and gain. The attenuation is caused by two-photon absorption, polaron absorption, and the appearance of higher diffraction orders. It is the diffraction of the strong pump pulse into the weak probe which is responsible for amplification.

A simplified approach can be used to account for all these processes. It represents the normalized transmission of the probe pulse $T(\Delta t)$ as a product of two factors $A(\Delta t)$ and $G(\Delta t)$ that describe the fractional changes of transmission which are due to losses and gain, respectively. As all losses can only decrease the transmission, A should be smaller than unity but should remain always positive, $0 \leq A \leq 1$. The gain factor G is always larger than unity but it is limited by the intensity ratio R of the interacting pulses $1 \leq G \leq R + 1$, as energy can be transferred to the probe only from the pump pulse.

For further analysis, the energy gain is introduced as an experimentally measurable quantity

$$G(\Delta t) = \frac{T_{\parallel}(\Delta t)}{T_{\perp}(\Delta t)} = \frac{A(\Delta t)G(\Delta t)}{A(\Delta t)}, \tag{3}$$

i.e., the ratio of the transmission with identically polarized $T_{\parallel}$ (gain and losses) and cross-polarized $T_{\perp}$ (losses only) pump and probe pulses. According to Eq. (3), the ratio $T_{\parallel}(\Delta t) / T_{\perp}(\Delta t)$ is not affected by nonlinear absorption $A(\Delta t)$. Such a treatment is justified under the assumption that both, the instantaneous losses for TPA as well as losses for residual polaron absorption, exhibit a negligible polarization dependence [36, 43]. A small difference in $A(\Delta t)$ for ordinary and extraordinary pump waves can therefore be neglected. The pulse delay dependence of the gain $G(\Delta t)$ extracted in such a way is shown in the inset to Fig. 2; the value of $G^{\max} = (4.4 \pm 0.2)$ is reached in the vicinity of $\Delta t = 0$.

The gain intensity dependence as well as its intensity ratio dependence are important characteristics for the identification of a particular coupling process. Figure 3 shows the gain $G^{\max}$ as a function of peak intensity for the shortest pulses used ($\tau_c \simeq 80$ fs) and two different ratios of the peak intensities R. A nonlinear increase of the gain is observed for intensities I below 300 GW/cm^2 for both values of R. Within the quite large error bars the data can be fitted by a $I^{2.5}$ dependence.

The gray area in Fig. 3 represents the possible range of gain variation only for the black squares ($R \approx 1000$). Both dependences, for $R \approx 1000$ and $R \approx 100$, show an obvious tendency to saturation of the gain at high intensities, with saturation level decreasing for $R \to 1$.

Figure 4 shows the gain $G(\Delta t = 0)$ as a function of the input pump/probe peak intensity ratio R while keeping the total peak intensity I constant. The logarithmic plot used here underlines

Optics EXPRESS

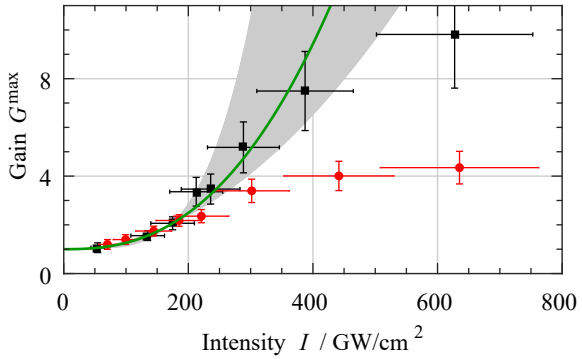

Fig. 3. Gain G^{max} versus total pulse peak intensity I. Black and red symbols show the data for the intensity ratios $R \approx 1000$ and $R \approx 100$, respectively, for pulses with durations $\tau_c = (80 \pm 5)$ fs and beam radii $r = (55 \pm 5)$ µm. For intensities below 300 GW/cm^2 the measured data can be fitted with G^{max}-1 $\propto I^m$. For R = 1000 such a fit gives m = 2.5 (green line); the gray shaded area is limited by functions with the exponents 2 < m < 4.

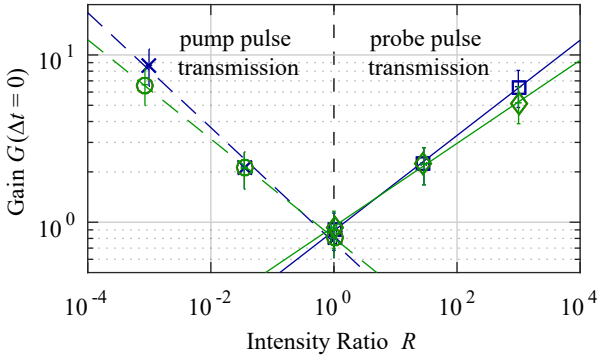

Fig. 4. Gain $G(\Delta t = 0)$ versus peak intensity ratio R in a log-log plot. Right and left branches show the experimentally measured gain for weak probe and weak pump pulses, respectively. The total peak intensity of two pulses is $I \approx 630$ GW/cm^2 (blue) and $I \approx 380$ GW/cm^2 (green) with pulses duration $\tau_c = (80 \pm 5)$ fs and beam radii $r = (55 \pm 5)$ µm. Solid and dashed lines are plotted as a guide to the eye.

that the energy flows always from the strong to the weak pulse. For $R \leq 1$ the peak intensity of the probe pulse becomes larger than that of the pump, and the measured gain G is related here to the normalized pump pulse transmission. It is obvious that the gain $G(\Delta t = 0)$ increases with growing R and vanishes for equal peak intensities $R = 1$ for a weak probe pulse. Similarly, for $R \leq 1$ the gain of a weak pump pulse increases with R^{-1}. The branches for $R \leq 1$ and $R \geq 1$ are basically symmetric, with approximately the same absolute exponent for the intensity ratio dependence $G \propto R^{\pm 0.3}$. The fact that the measured values of gain $G(\Delta t = 0)$ at $R = 1$ are roughly 10% smaller than unity indicates that additional losses exist besides those already accounted for TPA and polaron absorption. These losses are due to the light going into higher orders of diffraction. They become the most significant for a 1 : 1 intensity ratio of the recording pulses.

The measured dependences of gain [Figs. 3 and 4] are typical for transient beam coupling [37–39] what will be explained in details in section 4, Discussion.

Optics EXPRESS

3.2. Coupling of pulses with equal energies

As it was demonstrated in the previous subsection no energy redistribution occurs between two perfectly synchronized pulses ($\Delta t = 0$) with equal energies [see Fig. 4]. In what follows we show that even with $R = 1$ an energy redistribution becomes possible when a temporal mismatch between two frequency-chirped pulses is introduced. Two pulses with equal energies are chosen in these experiments to avoid any possible energy flow from a strong to a weak pulse.

It is known that the removal of frequency degeneracy of two recording waves may result in a strong intensity coupling, both for interactions of continuous waves [2] and sub-picosecond pulses [13,21,44]. The pulse delay of two otherwise identical pulses with a linear frequency chirp $\dot{\omega}$ [see Eq. (2)] is used in our further experiments to adjust a controllable frequency detuning Ω. Both pulses, still called pump and probe in a formal way, have time-dependent frequencies $\omega_{\mathrm{pr,pu}}(t) = \omega_0 + \dot{\omega}t$. Thus, for any non-zero Δt an instantaneous frequency detuning $\Omega(\Delta t)$ appears that does not depend on time:

$$\Omega(\Delta t) = \omega_{\mathrm{pr,pu}}(t - \Delta t) - \omega_{\mathrm{pu,pr}}(t) = -\dot{\omega} \cdot \Delta t \,. \tag{4}$$

Figure 5(a) gives a representative example of the pulse delay dependence of the normalized transmission $T_{\mathrm{pr,pu}}(\Delta t)$ for two identical pulses, i.e., with the same peak intensity ($R = 1$), chirp coefficient, polarization, pulse duration, beam radius, central wavelength, spectral width and symmetrical angles of incidence [as shown in Fig. 1]. The labeling of pulses as pump and probe is a matter of convention here because both pulses are indistinguishable. However, the sign of the temporal delay is chosen in such a way that for positive values of Δt, the pump pulse passes the sample prior to the probe pulse.

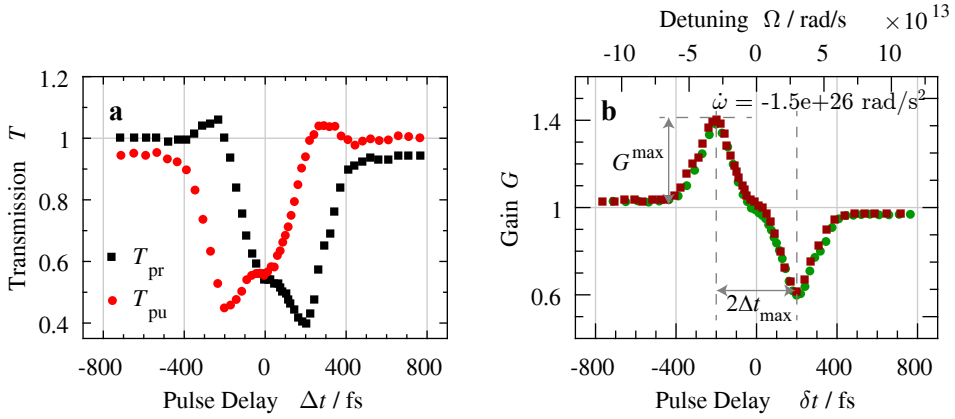

Fig. 5. Pulse delay dependences of (a) normalized transmission $T(\Delta t)$ for pump and probe pulses and (b) gain $G(\delta t)$ evaluated according Eq. (5) (with flipped curve $\delta t = -\Delta t$ for the data T_{pu}). Each pulse has an energy of $W = (5.1 \pm 0.1)\,\mu\mathrm{J}$, a pulse duration of $\tau_c \approx 235\,\mathrm{fs}$ and a bandwidth of $\Delta\omega = 3.7 \times 10^{13}$ rad/s. The beam radii are $r \approx 160\,\mu\mathrm{m}$ and the sum of the peak intensities of both pulses is $I \approx 100\,\mathrm{GW/cm^2}$.

First of all, in Fig. 5(a) a mirror symmetry is obvious for the two curves that define pump and probe transmission. This symmetry could be expected because the advanced pulse becomes the delayed pulse (and vice versa) when the pulse temporal mismatch Δt changes its sign. For this reason the axis of symmetry can be used to find the position of perfect temporal overlap of the pulses $\Delta t = 0$. At this particular position the transmission values are nearly the same for both pulses, thus indicating no energy redistribution. This is in agreement with the data of Fig. 4 for $G(\Delta t = 0)$ at $R = 1$, where only additional losses and no energy redistribution have been detected.

Optics EXPRESS

As distinct from the data of Fig. 2, the maximum of the pulse transmission T is reached now at a much longer pulse delay; it approaches 1.1 roughly at $\Delta t \simeq \pm 260$ fs. The transmission of the second pulse shows a pronounced dip at the same time, thus indicating that the energy gain of one pulse is caused by a depletion of the other one.

In this new set of measurements with $R = 1$ the transmission is measured for both interacting pulses simultaneously. This allows for estimating the gain G without an additional measurement of the transmission for orthogonally polarized pulses. New expressions for G are derived instead of Eq. (3), still maintaining the same definition of the normalized transmission as a product of loss and gain factors $T(\Delta t) = A(\Delta t)G(\Delta t)$. It is assumed, however, that the pulse delay dependent loss factors are the same for both pulses $A_{\mathrm{pr}}(\Delta t) = A_{\mathrm{pu}}(\Delta t)$. As a consequence, the transmission ratio of both pulses appears to be equal to the ratio of the pulse energy gain $T_{\mathrm{pr}}(\Delta t)/T_{\mathrm{pu}}(\Delta t) = G_{\mathrm{pr}}(\Delta t)/G_{\mathrm{pu}}(\Delta t) = P(\Delta t)$ and it becomes possible to quantify the gain factors as follows:

$$G_{\mathrm{pr}}(\Delta t) = \frac{2P(\Delta t)}{1 + P(\Delta t)} \quad , \quad G_{\mathrm{pu}}(\Delta t) = \frac{2}{1 + P(\Delta t)} \quad . \tag{5}$$

The G values defined by Eq. (5) cannot exceed $G = 2$ for both interacting pulses, what corresponds to a total energy transfer from one pulse to the other. Therefore, the "gain" of the depleted pulse cannot become smaller than $G = 0$; $G = 1$ still indicates no pulse amplification. Because of energy conservation the sum of these two gain parameters should always be constant $G_{\mathrm{pr}}(\Delta t) + G_{\mathrm{pu}}(\Delta t) = 2$.

Figure 5(b) represents the time delay dependence of the gain G replotted from the data of Fig. 5(a) according to Eq. (5). A new variable δt is introduced to pin the gain measured for the delayed pulse always to positive values of δt. Thus, δt coincides with Δt for the black curve of Fig. 5(a) and is inverted in its sign for the red data points $\delta t = -\Delta t$. This change of the pulse delay variable in Fig. 5 does not only underline the similarity of the shown curves, it further allows for adding a second axis for the frequency detuning Ω as estimated from Eq. (4). The data of Fig. 5(b) indicate an energy flow from the delayed to the advanced pulse, i.e., from the pulse with higher frequencies to the pulse with lower frequencies. It should be noted that the coupling direction is insensitive to the $LiNbO_3$ sample rotation to 180° along the z-axis as well as along the x-axis. The gain extrema are separated by $2\Delta t_{\mathrm{max}} \approx 400$ fs and the maximum gain reaches $G^{\mathrm{max}} \approx 1.4$. This pulse delay, that ensures the strongest coupling, corresponds to a certain fixed frequency detuning of $\Omega_{\mathrm{max}} = 3.0 \times 10^{13}$ rad/s.

The assumption $A_{\mathrm{pr}}(\Delta t) = A_{\mathrm{pu}}(\Delta t)$ that has been formulated when deriving Eq. (5) can be justified as follows: within the area of strong temporal overlap of two pulses, $|\Delta t| \leq 2\tau_{\mathrm{c}}$, the dominant losses are due to two-photon absorption and diffraction into higher orders, whereas the contribution of residual absorption from small polarons is much smaller. The latter can only be seen for large values of $|\Delta t|$ with transmission values slightly below unity. Because of the small magnitude of the polaron absorption in comparison to instantaneous losses, its impact on the gain evaluation should be minor. This estimate is supported by the data of Fig. 5(b), where the deviation of the gain from unity is hardly detectable for large pulse delays $|\delta t|$, and is much smaller than the maximum gain.

In the measurements presented above, the sign of the chirp coefficient is imposed to be negative $\dot{\omega} < 0$, resulting from the negative dispersion introduced by the grating compressor. To verify the sensitivity of the energy transfer direction to the sign of the frequency chirp, the latter was reversed to become positive $\dot{\omega} > 0$ by profiting from the material dispersion of a double prism compressor (N-SF11 dense flint glass).

In Fig. 6 the left and right graphs show the time delay dependences of G for pulses with negative and positive chirp coefficients $\dot{\omega}$, respectively. It is obvious that the flip of the chirp sign results in a change of the energy flow direction, whereas their extrema still occur roughly at same detunings Ω. The difference in gain magnitudes in Fig. 6(a) and Fig. 6(b) might be caused

Optics EXPRESS

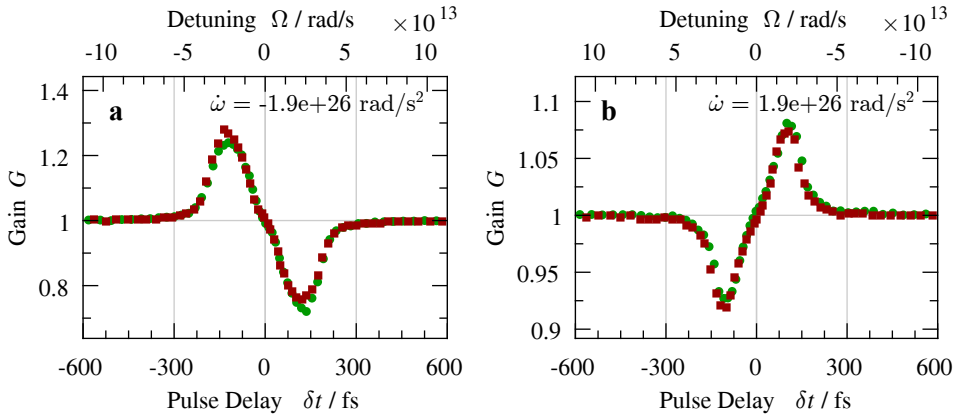

Fig. 6. Pulse delay dependence of gain $G(\delta t)$ for (a) pulses with a negative frequency chirp and energies $W = (2.6 \pm 0.1)\,\mu$J and (b) pulses with a positive frequency chirp and energies $W < 2\,\mu$J. Identical pulses are used, with central wavelengths $\lambda = 590\,$nm, bandwidths of $\Delta\omega = 4.0 \times 10^{13}$ rad/s and durations $\tau_c \approx 200\,$fs. The pulse frequency detuning Ω estimated according to Eq. (4) is shown as the upper x-axis. Red and green colors mark two interacting pulses.

by different pulse energies. It should be mentioned that these measurements are performed at a higher wavelength ($\lambda = 590\,$nm) than previous measurements. The two-photon absorption coefficient is smaller for higher wavelength and the residual absorption of photogenerated small polarons is reduced, too. As a consequence, the deviation of the gain from unity in a range of large pulse delays becomes basically undetectable.

The position of gain extrema can be used to determine the optimum frequency detuning for the pulses to ensure the highest energy transfer: $\Omega_{max} = 2.4 \times 10^{13}$ rad/s for Fig. 6(a) and $\Omega_{max} = 2.0 \times 10^{13}$ rad/s for Fig. 6(b). The measured dependences of gain are obviously antisymmetric (odd) functions, i.e., the change of the detuning sign results in the inversion of the energy transfer direction. This leads to the conclusion that in this set of measurements the reason of the pulse energy coupling is the frequency difference of the two pulses.

3.3. Pulse duration dependence

The pulse-delay dependences of gain, similar to that shown in Fig. 5(b), are collected in the next set of experiments for negatively chirped pulses of different durations τ_c. A double grating pulse stretcher is used to control τ_c, sketched in Fig. 1. The measured data are used to plot in Fig. 7(a) the dependence of the largest values of the gain $G^{max}(\tau_c)$ versus pulse duration (red dots). In the same Fig. 7(a) one can see how the temporal mismatch of the interacting pulses $\Delta t_{max}(\tau_c)$, which is necessary to ensure G^{max}, varies with the pulse duration (black squares).

The maximum gain increases with the pulse duration up to $\tau_c \approx 300\,$fs; for longer pulses it saturates at $G^{max} \approx 1.45$. At the same time, the pulse duration dependence of the largest gain position is linear: $\Delta t_{max} = \epsilon\tau_c$, and can be fitted with a slope of $\epsilon \simeq 0.9$.

According to Eq. (2), the chirp coefficient $\dot{\omega}$ depends on the chirped pulse duration τ_c, as it is shown by the gray shaded curve in Fig.7(b). For long pulses $\dot{\omega}$ is inversely proportional to the pulse duration τ_c (see hyperbolic asymptote shown with black dots); it decreases, however, in the vicinity of the Fourier-limited pulse duration $\tau_0 \approx 75\,$fs. The measured temporal mismatch, which is necessary for reaching the maximum gain Δt_{max}, can be used for the evaluation of a corresponding frequency detuning $\Omega_{max} = -\dot{\omega}\Delta t_{max}$. The result is plotted with blue squares in Fig. 7(b) for different pulse durations τ_c. For long pulses with $\tau_c > 300\,$fs the largest gain is

Optics EXPRESS

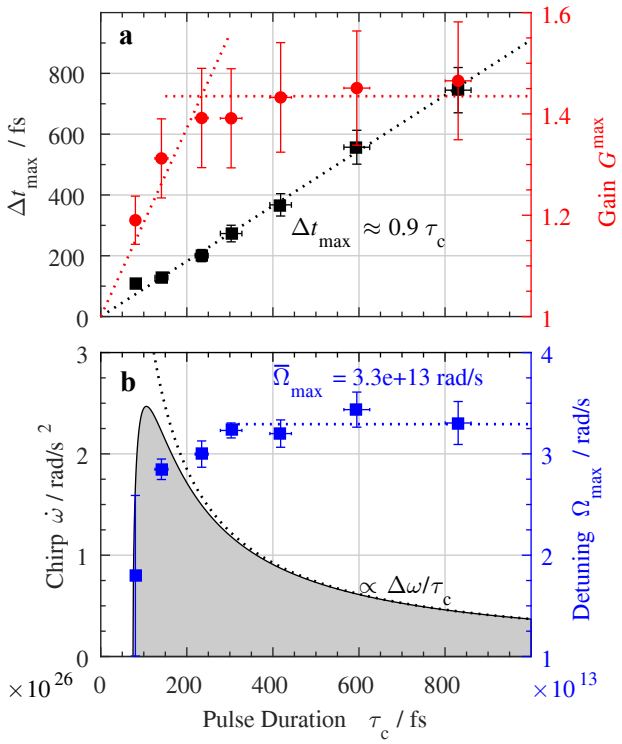

Fig. 7. (a) Pulse duration dependences of largest gain G^{max} (red dots) and pulse temporal mismatch that ensures this largest gain Δt_{max} (black squares). The red dotted lines are guiding the eye, while the black dotted line is a linear fit. (b) Pulse duration dependences of the chirp coefficient $\dot{\omega}$ (gray shaded curve) and pulse frequency difference that provides the maximum gain Ω_{max} (blue squares), extracted from the data plotted in (a). The blue dotted line represents $\bar{\Omega}_{max}$, the mean value of data above $\tau_c = 300$ fs. A hyperbolic dependence $\propto 1/\tau_c$ (black dots) shows the asymptotic behavior of the chirp coefficient $\dot{\omega}$ for long pulses. Both pulses have the same central wavelengths $\lambda = 488$ nm and bandwidths of $\Delta\omega = 3.7 \times 10^{13}$ rad/s.

always reached roughly at the same frequency detuning $\bar{\Omega}_{max} = 3.3 \times 10^{13}$ rad/s (dotted blue line); this optimum detuning value decreases for shorter pulses. The same constant value of Ω_{max} can be extracted by combining Eq. (2) and Eq. (4):

$$\Omega_{max} = \frac{\Delta\omega}{\tau_c}\epsilon\tau_c = \Delta\omega\epsilon \quad . \tag{6}$$

Furthermore, the ϵ value close to unity indicates that for a maximum gain the pulses are temporally separated by almost their FWHM.

Thus, the presented data confirm the conclusion of subsection 3.2 that the reason of the energy redistribution between two identical pulses nests in their frequency difference. It is shown in addition that the most efficient coupling occurs always at the same optimum detuning $\bar{\Omega}_{max}$ within a rather wide range of pulse durations.

3.4. *Coupling of frequency-shifted pulses with different energies*

The results of the previous subsections allow for the conclusion that the energy transfer can appear either because of a difference in incident pulse energies (subsection 3.1) or a difference in

Optics EXPRESS

frequencies of the two pulses (subsections 3.2 and 3.3). Whereas the origin of energy exchange for the interaction of delayed chirped pulses of equal energies can be unambiguously attributed to self-diffraction from the moving grating, caused by the frequency difference of the pulses, the non-zero gain of temporally matched, nearly Fourier-transform-limited pulses with different energies requires a more careful analysis.

At first glance, the chirp coefficient is close to zero for Fourier-transform-limited pulses and one cannot expect the removal of frequency degeneracy within the range of pulse temporal mismatch of Fig. 2. At the same time we are dealing with pulses that are not monochromatic. They possess spectra with FWHM $(3.7 - 4.0) \cdot 10^{13}$ rad/s, that exceed the optimum detuning $\Omega_{max} = (2.0 - 3.3) \cdot 10^{13}$ rad/s [see Fig. 6(b)]. Therefore, it is not excluded that a "blue" spectral slice (with a higher frequency) in one pulse may interact with a "red" slice of lower frequency in the other pulse, and vice versa. This will not result in energy redistribution for identical pulses with the same energies because the contradirectional energy flows will fully compensate for each other. Such compensation becomes, however, only partial if two pulses have different energies; the direction of the resulting energy flow being always from the strong pulse to the weak one [cf. Fig. 4].

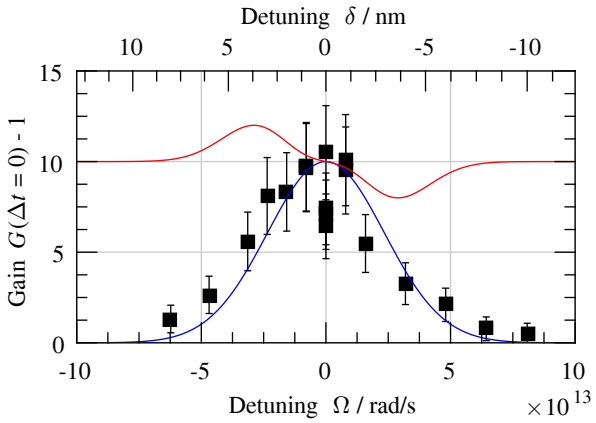

Fig. 8. Gain of a weak probe pulse G-1 versus probe-pump pulse frequency detuning $\Omega = \omega_{pr} - \omega_{pu}$ (black squares). Blue and red solid lines show qualitatively the expected contributions to the overall gain from transient beam-coupling and coupling from a moving grating (see text).

To clarify a possible influence of the pulse bandwidth and to identify an interaction process which is responsible for the coupling between the weak and strong pulses we have performed an additional experiment with pulses from two independently tunable OPAs. The gain of the weak probe is studied with pump and probe pulses that are matched in time but have deliberately detuned central frequencies $\Omega = \omega_{pr} - \omega_{pu}$.

As it was mentioned above, the enhancement of the "red" component of the weak pulse spectrum might be larger than the depletion of its "blue" component thus bringing overall amplification of the weak pulse. Assuming this explanation is valid, one can expect an increase of the measured gain for probe pulses which are gradually tuned to smaller frequencies until Ω_{max} is reached. For increasing probe frequency, on the contrary, the gain is expected to drop down, becoming even smaller than unity at a certain positive Ω. Thus, one should see a strongly asymmetric detuning dependence of the gain, that is qualitatively similar to the slightly deformed dependence shown in Fig. 5(b).

The measured detuning spectrum of $G - 1$ (filled squares) is depicted in Fig. 8. The wavelength of the pump pulse $\lambda_{pu} = 488$ nm is fixed, while the probe pulse wavelength λ_{pr} is varied. The

Optics EXPRESS

wavelength detuning $\delta = \lambda_{pr} - \lambda_{pu}$ is added as the second x-axis on the top.

The detuning dependence of Fig. 8 is only slightly asymmetric, with the maximum shifted to longer wavelength of the probe pulse (negative frequency detuning). It looks like a superposition of a dominating bell-shaped (even) and an odd function with a smaller amplitude. These two functions are shown by blue and red solid lines for guiding the eye, red line being up-shifted to the maximum of the blue one.

Thus, we can conclude that self-diffraction from a moving grating that is recorded by the "red" spectral component of the weak pulse and the "blue" spectral component of the strong pulse does exist and manifests itself in a slight asymmetry of the spectrum shown in Fig. 8. At the same time, the dominating process responsible for coupling of weak and strong pulses in this experiment and all experiments described in subsection 3.1 is the transient energy transfer [37, 38].

4. Discussion

All presented results clearly show a net gain of a probe pulse when it is interacting with a pump pulse within congruent, nominally undoped lithium niobate. This gain cannot be a consequence of sample bleaching because of a very small linear absorption of the used sample in the blue-green spectral domain ($\alpha_{488} \leq 1\,\mathrm{cm}^{-1}$). Moreover, to become clearly visible ($T > 1$) the gain should overcome two-photon absorption, which is quite pronounced within the intensity range of the pulses used in these experiments.

As we mentioned already, we attribute the pulse coupling effects and appearance of higher diffraction orders to self-diffraction from one and the same dynamic grating. Thus, the measured efficiency of diffraction into the first non-Bragg order $\eta \approx 0.01$ allows for estimating roughly the refractive-index modulation $\Delta n \geq (\sqrt{\eta}\lambda/\pi\ell)$. With a sample thickness of $\ell = 280\,\mu\mathrm{m}$ and a light wavelength of $\lambda \simeq 0.5\,\mu\mathrm{m}$ we get Δn on the order of 10^{-4}. Taking into account Gaussian transverse intensity distribution, a nonuniform distribution within the sample thickness because of TPA and its nearly Gaussian temporal variation, the peak value of Δn should be much larger than 10^{-4} and quite strong coupling can be expected. At the same time, to ensure an efficient beam-coupling, the recorded grating should have a component which is $\pi/2$ shifted in phase with respect to the recording fringes [1–3]. The use of various inertial refractive $\chi^{(3)}$ nonlinearities can ensure the necessary phase shift between the grating and the fringes if two interacting waves differ in temporal frequencies and thus form a moving fringe pattern. The response of the inertial nonlinear medium is time-delayed. Therefore, the moving fringes produce a grating which propagates in space with the same speed as the fringes but with the extrema that do not coincide with the maxima of the intensity.

In lithium niobate, phase and/or amplitude gratings can be recorded by several known processes when using femtosecond excitation. The two-photon absorption and optical Kerr effect nonlinearities which have been considered previously as origin of dynamic grating recording [32, 33] are essentially instantaneous. Therefore, self-diffraction from relevant dynamic gratings cannot result in the intensity coupling of the recording waves. The TPA grating can only decrease the intensity of the probe beam while an instantaneous refractive index grating from the optical Kerr effect by definition can never be shifted in space with respect to the light fringes. Other known nonlinearities of $LiNbO_3$ are caused by photogeneration of excitons, free carrier and small polarons [29, 32, 35] as also by excitation of optical phonons. All mentioned nonlinearities are refractive and inertial and therefore can be involved in pulse coupling. Additional studies will be necessary to identify the origin of the nonlinearity which is responsible for pulse coupling in our experiments.

The intensity redistribution between two waves which are recording a moving index grating [2, 3, 6, 11, 13] is a well known phenomenon. It was reported for laser filaments in gases [6, 13] and in liquids [11] for subpicosecond pulses. Being not qualitatively new, this type of coupling is revealed now for the first time in a solid-state nonlinear material and shown to be very efficient.

Optics EXPRESS

The quantitative data for pulse coupling in a $LiNbO_3$ sample with an interaction length of only 280 μm are quite impressive: one order of magnitude amplification of the weak probe pulse energy [Fig. 3] and nearly 10% net enhancement of one of two pulses with same input energies [Fig. 6] are demonstrated. The energy is transferred from the high frequency pulse to the low frequency one with an optimum detuning of $\Omega \approx 3 \times 10^{13}$ rad/s. The frequency detuning dependences of gain G given in Fig. 6 are obviously odd functions, qualitatively similar to

$$g \propto g_0 \frac{\Omega\tau_c}{1+\Omega^2\tau_c^2} \quad , \tag{7}$$

predicted by simple models for lossless media [see, e.g., Eq. (129) of [22]]. The gain factor g defines here the steady-state exponential gain of a weak probe beam, $I_{pr} \simeq I_{pr}^{(0)} \exp(g\ell)$. It can be expressed via G used in this article, $g \approx (G-1)/\ell$, ℓ standing for the interaction length. The deviation of experimental dependences of Fig. 6 from the simple form expressed by Eq. (7) might be helpful for the identification of the physical origin of nonlinearity, most probably related to certain crystal lattice resonances.

Let us compare now the manifestations of weak-to-strong pulse coupling in our experiment with the results of the transient beam-coupling model [37]. Being developed for continuous wave interaction, this model predicts no intensity coupling in the steady-state and an appearance of probe wave amplification during a time interval comparable to the grating build-up or decay time τ_r. The intensity is always transferred from a strong wave into a weak one. For the initial stage of recording, $t \ll \tau_r$, the gain increases nonlinearly with intensity I, sample thickness ℓ and time t. The relationship between the relative changes of the probe intensity I_{pr} and parameters mentioned above is as follows [37]:

$$\frac{I_{pr}-I_{pr}^{(0)}}{I_{pr}^{(0)}} = 4\Phi^2\left[\frac{I_{pu}^{(0)}-I_{pr}^{(0)}}{I_{pu}^{(0)}+I_{pr}^{(0)}}\right]\exp\left(-\frac{t}{\tau_r}\right)\left[1-\left(\frac{t}{\tau_r}\right)-\exp\left(-\frac{t}{\tau_r}\right)\right]. \tag{8}$$

Here, $\Phi = k_0\Delta n\ell/2\cos\theta$ stands for the light-induced phase modulation in a sample with a thickness ℓ, $k_0 = 2\pi/\lambda_0$ is a wavenumber, θ is a half-angle between the interacting beams and all superscripts (0) indicate the transmitted intensity with no second wave present. In fact, Eq. (8) gives the expression for the temporal variation of the instantaneous transmission $[T(t)-1]$ or instantaneous gain $[G(t)-1]$.

Several assumptions in the above summarized theories prevent from a more quantitative description of the nonlinear interactions of ultrashort pulses: (*i*) the pulses have a particular temporal envelope which is quite different from a step-like onset in time of the pump intensity, considered in these theories, (*ii*) pulses with a Gaussian transverse intensity profile can hardly be treated in the plane-wave approximation, and (*iii*) the propagation effects are not considered in the existing theories. The analysis of the experimental data presented below allows, however, for confirming their qualitative agreement with the predictions of this simplified model.

First, it should be noted that the relationship of Eq. (8) was derived for photorefractive media in which Δn is independent of the light intensity, i.e., the gain is independent of the cw-laser beams intensity in an appropriate experiment. Taking into account that in the subpicosecond time domain the most probable processes of nonlinear index variation $\Delta n(I)$ in lithium niobate are caused by free-carriers or polarons generated via two-photon absorption [36] one can expect, even from Eq. (8), an experimental intensity dependence I^m with an exponent larger than 2. The measured gain of a probe pulse increases, as could be expected, superlinearly with the total peak intensity with $2 < m < 4$ [Fig. 3], showing an impact of the peak intensity ratio. For pulses with different peak intensities it is always the weak pulse that gains intensity [Fig. 4]. The intensity coupling disappears completely for equal peak intensities of both pulses $I_{pr} = I_{pu}$ or $R = 1$ [Fig. 4], if the pulses are perfectly matched in time. All these features permit to attribute the

Optics EXPRESS

coupling of the weak and strong pulses to a transient-type nonlinear interaction with an inertial phase grating involved [37, 38].

We claim, therefore, that two qualitatively different coupling processes are revealed in the experiments with grating-assisted pulse coupling in $LiNbO_3$, one with a steady-state gain from a moving grating recorded by pulses with different frequencies and the other with a transient gain of a weak pulse in presence of a strong pump pulse with the same frequency. The experimental conditions were selected in a way to inhibit one of these two processes and to study the other one in more detail. The coupling of pulses with equal energies is, in the first instance, feasible because of the frequency difference of two temporally mismatched pulses while the transient beam-coupling can manifest itself in a small-signal amplification of pulses that are perfectly matched in time.

The physical processes that are responsible for the optical nonlinearities at the origin of grating recording itself are not yet established. Some qualitative considerations allow for formulating the requirements for their parameters. In order to observe a transient energy transfer, as it is known, the decay time of the nonlinearity should be longer compared to the pulse duration. For efficient coupling of pulses that are non-degenerated in frequency this time should be, on the other hand, comparable or shorter than the pulse duration. Thus, a good candidate for dominating inertial nonlinearity is the photoexcitation of electron-hole pairs which are further responsible for the appearance of (self-trapped) excitons and/or small, strong-coupling polarons. The nonlinearity which is contributing for coupling from moving gratings might be related to the inherent optical resonances of the $LiNbO_3$ lattice.

5. Conclusion

The experimental study of the dynamic grating assisted energy transfer between two sub-picosecond pulses reveals that this process can be quite efficient in $LiNbO_3$. The weak probe pulse can be amplified more than 10 times and the redistribution of energy between two pulses of equal intensities might approach 50% of each pulse energy. This efficient coupling is accompanied, however, by a considerable attenuation of both pulses because of two-photon absorption.

The analysis of the whole scope of experimental data leads to the conclusion that at least two different coupling processes are strongly involved, both related to self-diffraction from the recorded dynamic phase grating. The first coupling process results from the appearance of a moving grating which is shifted with respect to the moving fringe pattern, induced by two pulses with different frequencies. The frequency shift may either be introduced deliberately by using pulses from two different OPAs with adjustable wavelengths, or it may appear if the grating is recorded by two frequency chirped and temporally mismatched pulses from a single OPA. The second process manifests all characteristic features of the transient energy transfer which was first reported for cw and is closely related to stimulated Rayleigh-wing scattering. While the first process ensures an efficient unidirectional coupling between two pulses regardless of their intensity ratios, the second one always provides an efficient energy flow from the stronger to the weaker pulse.

Funding

Deutsche Forschungsgemeinschaft (DFG) (IM 37/11-1, INST 190/165-1 FUGG); Open Access Publishing Fund of Osnabrück University.

Acknowledgment

The authors gratefully acknowledge crystal preparation by K. Polgár and coworkers at the Wigner Research Centre for Physics, Budapest.

Optics EXPRESS

References

1. V. L. Vinetskii, N. V. Kukhtarev, S. G. Odulov, and M. S. Soskin, "Dynamic self-diffraction of coherent light beams," Sov. Phys. Usp. **22**, 742–756 (1979).
2. L. Solymar, D. J. Webb, and A. Grunnet-Jepsen, *The Physics and Applications of Photorefractive Materials* (Clarendon, 1996).
3. P. Yeh, *Introduction to Photorefractive Nonlinear Optics*, Wiley series in pure and applied optics (Wiley, 1993).
4. P. Günter and J.-P. Huignard, eds., *Photorefractive Materials and Their Applications*, Vol. 1–3, Springer series in Optical Science, (Springer, 2007).
5. S. Smolorz and F. Wise, "Femtosecond two-beam coupling energy transfer from Raman and electronic nonlinearities," J. Opt. Soc. Am. B **17**, 1636–1644 (2000).
6. A. C. Bernstein, M. McCormick, G. M. Dyer, J. C. Sanders, and T. Ditmire, "Two-beam coupling between filament-forming beams in air," Phys. Rev. Lett. **22**, 13–16 (2009).
7. J. K. Wahlstrand, J. H. Odhner, E. T. McCole, Y.-H. Cheng, J. P. Palastro, R. J. Levis, and H. M. Milchberg, "Effect of two-beam coupling in strong-field optical pump-probe experimets," Phys. Rev. A **87**, 053801 (2013).
8. R. L. Sutherland, "Energy transfer between incident laser and elastically backscattered waves in nonlinear absorption media," Opt. Express **13**, 9788–9795 (2005).
9. Y. Zhao, T. E. Witt, and R. J. Gordon, "Efficient energy transfer between laser beams by stimulated Raman scattering," Phys. Rev. Lett. **103**, 173903 (2009).
10. X. Yang, J. Wu, Y. Tong, L. Ding, Z. Xu, and H. Zheng, "Femtosecond laser pulse energy transfer induced by plasma grating due to filament interaction in air," Appl. Phys. Lett. **97**, 071108 (2010).
11. B. D. Stryker, M. Springer, C. Trendafilova, X. Hus, M. Zhi, A. A. Klolomenskii, H. Shroeder, J. Strohbaber, G. W. Kattawar, and A. V. Sokolov, "Energy transfer between laser filamentrs in liquid methanol," Opt. Lett. **37**, 16–18 (2012).
12. C. Gong, Y. Zheng, Z. Zheng, C. Li, X. Ge, R. Li, and Z. Xu, "Energy trsnsfer between few-cycle laser filamentrs in air," Appl. Phys. Lett. **101**, 251111 (2012).
13. Y. Liu, M. Durand, S. Chen, A. Houdard, B. Prade, B. Forrestier, amd A. Mysyrowicz, "Energy exchange between femtosecond laser filaments in air," Phys. Rev. Lett. **105**, 055003 (2010).
14. H. J. Eichler, D. Langhans, and F. Massmann, "Coherence peaks in picosecond sampling experiments," Opt. Commun. **50**, 117–122 (1984).
15. C. W. Luo, Y. T. Wang, F. W. Chen, H. C. Shin, and T. Kobayashi, "Eliminate coherence spike in reflection-type pump-probe measurements," Opt. Express **17**, 11321-11327 (2009).
16. N. Tang and R. L. Sutherland, "Time-domain theory for pump-probe experiments with chirped pulses," J. Opt. Soc. Am. B **14**, 3412–3423 (1997).
17. F. Gires, "Résultats expérimentaux sur la reflexion thermique stimulée," C. R. Acad. Sci. Ser. B **t. 266** 596–600 (1968).
18. M. E. Mack, "Stimulated thermal light scattering in the picosecond regime," Phys. Rev. Lett. **22**, 13–16 (1969).
19. G. Rivoire and D. Wang, "Dynamics of CS_2 in a large spectral bandwidth stimulated Rayleigh-wing scattering," J. Chem. Phys. **99**, 9460–9464 (1993).
20. K. D. Dorkenoo, D. Wang, N. P. Xuan, J. P. Lecoq, R. Chevalier, and G. Rivoire, "Stimulated Rayleigh-wing scattering with two-beam coupling in CS_2," J. Opt. Soc. Am. B **12**, 37–42 (1995).
21. A. Dogariu, T. Xia, D. J. Hagan, A. A. Said, E. W. Van Stryland, and N. Bloembergen, "Purely refractive transient energy transfer by stimulated Rayleigh-wing scattering," J. Opt. Soc. Am. B **14**, 769–803 (1997).
22. P. Yeh, "Two-wave mixing in nonlinear media," IEEE J. Quantum Electron. **25**, 484–517 (1989).
23. R. L. Sutherland, D. G.McLean, and S. Kirkpatrick, *Handbook of Nonlinear Optics*, 2nd ed. (CRC, 2003).
24. R. W. Boyd, *Nonlinear Optics*, 3rd ed. (Academic, 2008).
25. Y. Sivan, S. Rozenberg, A. Halstuch, and A.A. Ishaaya, "Nonlinear wave interactions between short pulses of different spatio-temporal extents," Sci. Rep. **6**, 29010 (2016).
26. R. Trebino, *Frequency-Resolved Optical Gating: The Measurement of Ultrashort Laser Pulses* (Springer Science & Business Media, 2012).
27. R. M. Brubaker, Q. N. Wang, D. D. Nolte, E. S. Harmon, and M. R. Melloch, "Steady-state four-wave mixing in photorefractive quantum wells with femtosecond pulses," J. Opt. Soc. Am. B **11**, 1038–1044 (1994).
28. H. Crespo, J. T. Mendonca, and A. Dos Santos, "Cascaded highly nondegenerate four-wave-mixing phenomenon in transparent isotropic condensed media," Opt. Lett. **25**, 829–831 (2000).
29. H. Badorreck, A. Shumelyuk, S. Nolte, M. Imlau, and S. Odoulov, "Doppler-shifted Raman-Nath diffraction from gratings recorded in $LiNbO_3$ with ultra-short laser pulses of different color," Opt. Mater. Express **6**, 517–522 (2015).
30. S. Odoulov, A. Shumelyuk, H. Badorreck, S. Nolte, K. M. Voit, and M. Imlau, "Interference and holography with femtosecong laser pulses of different colours," Nat. Commun. **6**, 5866 (2015).
31. D. Staebler and J. Amodei, "Coupled wave analysis of holographic storage in $LiNbO_3$," J. Appl. Pnys. **43**, 1042–1049 (1972).
32. H. T. Hsieh, D. Psaltis, O. Beyer, D. Maxien, C. von Korff Schmising, K. Buse, and B. Sturman, "Femtosecond holographgy in lithium niobate crystals," Opt. Lett. **30**, 2233–2235 (2005).
33. O. Beyer, D. Maxien, K. Buse, B. Sturman, H. T. Hsieh, and D. Psaltis,"Femtosecond time-resolved absorption processes in Lithium niobate crystals," Opt. Lett. **30**, 1366–1368 (2005).

Optics EXPRESS

34. J. P. Woerdman, "Some optical and electrical properties of a laser-generated free-carrier plasma in Si (Thesis)," Philips Res. Repts Suppl. #7 (1971).
35. P. Reckenthaeler, D. Maxien, Th. Woike, and K. Buse, "Separation of optical Kerr and free-carrier nonlinear responses with femtosecond light pulses in $LiNbO_3$ crystals," Phys. Rev. B **76**, 195117 (2007).
36. M. Imlau, H. Badorreck, and C. Merschjann, "Optical nonlinearities of small polarons in lithium niobate," Appl. Phys. Rev. **2**, 040606 (2015).
37. N. Kukhtarev, V. Markov, and S. Odoulov, "Transient energy transfer during hologram formation in $LiNbO_3$ in external electric field," Opt. Commun. **23**, 338–343 (1977).
38. V. Bryksin, A. Groznyj, V. Sidorovich, and D. Stasel'ko, "Efficient amplification of weak light beams by 3D dynamic holograms in media with thermal nonlinearity," Soviet Physics: Technical Physics Letters, **2**, 561 (1976).
39. B. Ya. Zel'dovich, N. F. Pilipetsky, and V. V. Shkunov, *Principles of Phase Conjugation* (Springer, 1985).
40. H. Badorreck, S. Nolte, F. Freytag, P. Bäune, V. Dieckmann, and M. Imlau, "Scanning nonlinear absorption in lithium niobate over the time regime of small polaron formation," Opt. Mater. Express **5**, 2729–2741 (2015).
41. F. Träger, *Springer Handbook of Lasers and Optics* 2nd ed. (Springer Science & Business Media, 2012), Chap. 12.
42. P. Yeh and A. Yariv, *Optical Waves in Crystals,* Wiley Series in Pure and Applied Optics (Wiley, 1984).
43. S. Sasamoto, J. Hirohashi and S. Ashihara, "Polaron dynamics in lithium niobate upon femtosecond pulse irradiation: Influence of magnesium doping and stoichiometry control," J. Appl. Phys. **105**, 083102 (2009).
44. A. Dogariu, and D. J. Hagan, "Low frequency Raman gain measurements using chirped pulses," Opt. Express **1**, 73–76 (1997).